Check for updates

Zigzag gas phases on holey adsorbed layers†

Hideaki Teshima,[ab] Naoto Nakamura,[a] Qin-Yi Li, [ID][ac] Yasuyuki Takata[cd] and Koji Takahashi [ID] *[ac]

We report for the first time a zigzag-shaped gas phase at a highly-ordered pyrolytic graphite/water interface. The novel shape of the gaseous domain is triggered by the holes of the underlying solid-like layers, which are composed of air molecules. Specifically, many holes were created by heating in the thin solid-like layers, which roughened them. The gas domains that formed on these layers deformed from circular to zigzag-shaped as the contact lines expanded while avoiding the holes of the underlying layers. We explained the formation and growth processes of these gas structures in terms of thin film growth, which varies with the mobility of the constituent molecules.

Introduction

Ultrathin gas layers at hydrophobic solid/liquid interfaces have attracted increasing attention, in particular relating to phenomena such as slippage of fluid flow on solid surfaces,[1] short-range hydrophobic interactions,[2,3] the pinning effect of surface nanobubbles,[4] and the promotion of gas hydrate formation.[5] Because accumulated gas molecules universally exist on hydrophobic surfaces,[2,6] revealing the underlying physics and their detailed behavior is crucial for understanding fundamental phenomena at solid/liquid interfaces, such as the aforementioned examples.

Until now, the three-dimensional visualization of the interfacial gaseous domains with sub-nanometer spatial resolution has only been achieved using atomic force microscopy (AFM). In 2000, spherical cap-shaped nanobubbles at a solid/liquid interface were first observed.[7,8] Subsequently, a number of studies reported the characteristic properties of these interfacial nanobubbles, such as their extraordinarily high contact angles,[7,9] long lifetime,[10] and superstability against disturbance,[11,12] and proposed a variety of theories to explain these

observations.[13–15] Furthermore, it has been revealed using AFM measurements that the accumulated gas molecules also form film-like structures with a height of a few nanometers or less. These structures include epitaxially-ordered layers,[4,16–21] disordered layers,[16,19,21] and micropancakes.[16,19,22–26] Recent studies have reported that each gas structure is layered in the following order on the underlying substrate surface: ordered layers, disordered layers, and micropancakes.[19] Moreover, these layers have been shown to exhibit different vertical and horizontal mobility, which has been attributed to the differences in the magnitude of the attractive van der Waals forces from the solid surface[16,19] and confinement in the hydration structures.[21]

For the measurement of these atomically thin layers, frequency-modulation (FM)-AFM has been used because of its higher measurement sensitivity[4,16–21] than the more conventional amplitude-modulation (AM)-AFM. However, we recently revealed[19] that although FM-AFM can be used to observe the mobility of micropancakes, it cannot precisely measure their morphology because they are dragged by the AFM probe owing to its small oscillation amplitude (less than a few nanometers). By contrast, we found that AM-AFM, in which the probe is oscillated at larger amplitudes, enables us to visualize the precise shape of micropancakes without dragging (see ESI Note S1†). On the basis of this discovery, we investigated the gas phases at the interface of highly-ordered pyrolytic graphite (HOPG) and pure water using AM-AFM. As we report in this paper, the interfacial gases were heated to induce the growth and associated changes in their morphology. We show micropancakes with a zigzag-shaped three-phase contact line—a structure that has never been reported for surface nanobubbles or other gaseous domains. Moreover, we produced disordered layers with a large number of holes. Similar to the initial stage of water vapor condensation under ambient conditions,[27] these novel molecular air layers grow in a layer-plus-island manner, although each layer exhibits distinctly different growth regimes. We present mechanisms to explain

[a]Department of Aeronautics and Astronautics, Kyushu University, Nishi-Ku, Motooka 744, Fukuoka 819-0395, Japan. E-mail: takahashi@aero.kyushu-u.ac.jp

[b]Department of Mechanical Engineering, Osaka University, 2-1 Yamadaoka, Suita 565-0871, Japan

[c]International Institute for Carbon-Neutral Energy Research (WPI-I2CNER), Kyushu University, Nishi-Ku, Motooka 744, Fukuoka 819-0395, Japan

[d]Department of Mechanical Engineering, Kyushu University, Nishi-Ku, Motooka 744, Fukuoka 819-0395, Japan

† Electronic supplementary information (ESI) available: The comparison of the structures of interfacial gases obtained by FM-AFM and AM-AFM, the details on AFM configuration and the preparation of the gas phases, the evaluation of the gas oversaturation, the observation of the ordered layers by FM-AFM and the broad area of the HOPG/pure water interface before and after heating by AM-AFM, Raman spectra obtained at HOPG in air, HOPG/degassed water interface, and HOPG/air-supersaturated water interface, and the AFM imaging of the HOPG surfaces in air and in degassed water. See DOI: 10.1039/d0ra08861g

the formation of these novel shapes and the difference in the growth regimes in terms of thin film growth.

Experimental methods

The AM mode of an SPM-9600 AFM (Shimadzu Corp., Japan) was used with SCANASYST-FLUID+ cantilevers (tip radius: 2–12 nm; Bruker Corp., USA). Before the measurements, the cantilevers were hydrophilized with oxygen plasma treatment (Plasma Reactor 500, Yamato Scientific, Japan) for 30 minutes to ensure the reliability and accuracy of the obtained images.[28] An HOPG (SPI-1 grade, 10 mm × 10 mm, Alliance Biosystems, Inc., Japan) substrate was fixed on the bottom of a glass liquid cell with a depth of ∼5 mm. A detailed configuration of the AFM setup is shown in ESI Note S2.† Interfacial gases were nucleated by the solvent-exchange method[7] using air-saturated ethanol and pure water. First, the HOPG was immersed in ethanol for several minutes. Then, the ethanol was thoroughly replaced by injecting water prepared by a water purifier (RFP742HA, Advantec, Japan). Because ethanol has a higher air solubility than water, this exchange creates an air-supersaturated condition in the liquid, resulting in the formation of nanoscale gas phases at the solid/liquid interface. The whole procedure was conducted in a clean room. A clean glass syringe and steel needle were used to avoid contamination.[29] Moreover, we have confirmed in previous studies[19,21,30] that the domains nucleated by our procedure are indeed gases and not contamination.

Heating was conducted using a ceramic heating unit (Shimadzu Corp., Japan) attached to the top of the scanner to promote the growth of interfacial gas phases through the decrease in gas solubility associated with the temperature rise. The temperature in the liquid during heating was monitored using a resistance thermometer. The temperature was first raised from the initial temperature (30 °C) to 60 °C over several minutes. Then, the heating unit was switched off and returned to the initial temperature over approximately 10 minutes. We confirmed that this procedure increased the gas oversaturation in the vicinity of the HOPG/water interface by measuring the contact angles of the surface nanobubbles[15] (shown in ESI Note S3†). AFM measurements were conducted at least one hour after being returned to the initial temperature to avoid thermal drift. All AFM measurements were conducted at the initial temperature. Simultaneous with the height images, phase images are also acquired using the AM mode. We compared the obtained images to detect the existence of the interfacial gas domains.

Results and discussion

Fig. 1(a) shows the height image of the HOPG/pure water interface before heating. As indicated by the red arrows, many micropancakes with a thickness of ∼1 nm were observed. Moreover, in the corresponding phase image (Fig. 1(b)), regions with different contrast from the bare HOPG surface were observed around the micropancakes, as indicated by the blue arrows. These regions were not clearly observed in the height image before heating (Fig. 1(a)) but became visible as flat domains with a thickness of ∼2 nm after heating (Fig. 1(c)). This

is because the micropancakes were too thin to detect before heating, but then increased to a detectable thickness owing to the adsorption of dissolved gas molecules promoted by the temperature rise. We consider these regions that appeared upon heating to be disordered layers because they form under the micropancakes.[19] Using high-sensitivity FM-AFM, we also confirmed the existence of ordered layers around the disordered layers, and that these ordered layers covered the entire HOPG surface (shown in ESI Note S4†). Therefore, there are three types of gas layer on the HOPG surface; namely, the ordered layer, the disordered layer, and the micropancakes.

The cross-sections of the same area before and after heating, indicated by the white dotted lines in Fig. 1(a and c), are shown in Fig. 1(e). The thickness of both the micropancakes and disordered layers increased upon heating. Furthermore, although the innermost ordered layers covered the entire HOPG surface (see ESI Note S4†), the coverage area of the overlying disordered layers and micropancakes was partial, even after heating (Fig. 1(c and d)). These indicate that the growth mode of the gas adsorbate changed from layer-by-layer (Frank–van der Merwe) growth to 3D-island (Volmer–Weber) growth. This sequence of layer-by-layer growth followed by the 3D island growth is commonly referred to as either layer-plus-island or Stranski–Krastanov (SK) growth mode.[31] Although the SK growth mode occurs in the initial stage of water condensation,[27] the growth regimes of each condensed gas layer in the present study were distinctly different from those of the water adlayers. Specifically, the surface of the disordered layers became rougher and many holes were created after heating, as indicated by the yellow arrows in Fig. 1(c and d) and in Fig. 1(e). By contrast, the micropancakes retained their smooth surface and contained a smaller number of holes than the disordered layers; however, their edges became zigzag-shaped, as indicated by the red lines in Fig. 1(d). Despite the similar binding energies of the gas/solid and water/solid interfaces, and the analogous growth to SK mode for water adsorption,[16,32,33] the aforementioned differences in the growth regime of each gaseous layer have never been observed for water adlayers.[27,34,35]

We have investigated HOPG/pure water interfaces three times under the same experimental conditions and could observe the zigzag micropancakes on holey adsorbed layers in all of them. Moreover, we also confirmed that these novel layers were formed over the entire HOPG surface, rather than in specific areas (see ESI Note S5†).

We propose a growth mechanism of these novel interfacial gas layers as follows. The growth regime of thin films through molecular accumulation is determined by the mobility of the constituent molecules.[36] It has been reported that the molecules constituting the ordered and disordered layers are immobile because of the strong interaction at the solid/gas interface,[16] resulting in solid-like behavior.[19,21] Because the strongly-adsorbed air molecules cannot diffuse on the surface to positions that make the local potential energy minimum, their growth regime is that of a self-affine random rough surface.[36] Consequently, the surface of the disordered layers becomes rough. In addition, the growth direction of the immobile layer is limited to the vertical direction because horizontal growth is
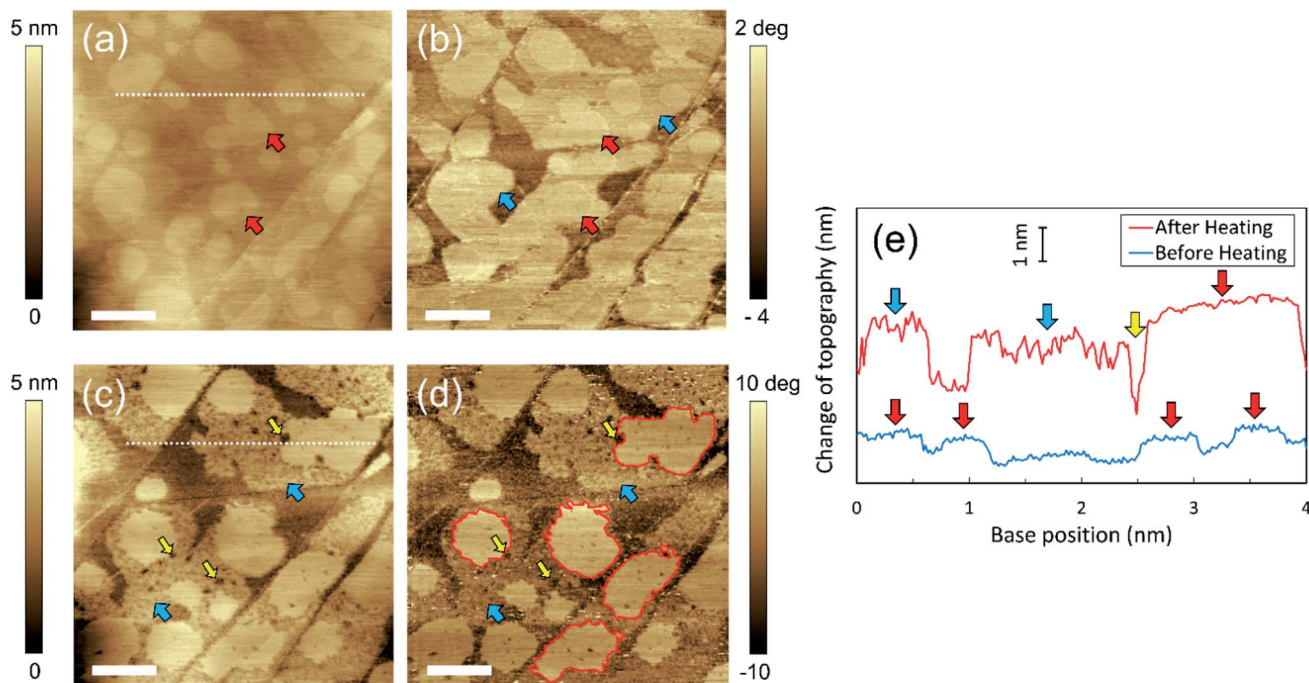
Fig. 1 Height images of the micropancakes and disordered layers (a) before and (c) after heating (5 μm × 5 μm). (b and d) Phase images corresponding to (a) and (c), respectively. The scale bars are 1 μm. (e) Cross sections corresponding to the white dotted lines in (a) and (c), showing the growth of the micropancakes and disordered layers. The red and blue arrows indicate the micropancakes and disordered layers, respectively. The yellow arrows indicate the holes in the disordered layers.

hard to occur with weak surface diffusion. Indeed, the area of the disordered layers estimated from Fig. 1 was almost the same before (79.3% ± 0.8%) and after (78.9% ± 0.6%) heating, which agrees with our interpretation. Furthermore, many holes are created in the disordered layers upon heating. We propose that the cause of their formation is that heating leads to the desorption as well as the adsorption of gas molecules. The physisorption of gas molecules to the HOPG surface is promoted by heating owing to the decrease in gas solubility. However, the desorption of them is also enhanced by heating because of the increase in the thermal energy of the adsorbed molecules, as described by the Arrhenius equation.[31] In addition, desorption is also induced when the liquid temperature returns to the initial temperature owing to the increase in gas solubility. Because the constituent gas molecules are strongly adsorbed and cannot diffuse on the HOPG surface, the holes remained unfilled. Therefore, the holes in the gaseous domains might be created during the desorption process.

In contrast with the strongly-adsorbed layers, micropancakes on them are mobile.[19] This is because the underlying ordered and disordered layers create a space between them and the HOPG surface, reducing the strength of the van der Waals interactions. Consequently, the constituent gas molecules spontaneously move to level the surface during growth owing to surface tension, resulting in the atomically flat shape shown in Fig. 1(e). Moreover, the gas accumulation causes the micropancakes to grow in both the horizontal and vertical directions. In fact, the coverage area of micropancakes in Fig. 1 increased from 32.4% ± 0.4% to 36.5% ± 0.2% upon heating. It was

previously reported that micropancake mobility is limited at the edges of the underlying adsorbed layers by the pinning effect of the three-phase contact line.[19] This pinning effect (i.e., an energy barrier preventing adatoms from descending to the lower layer) is called the Ehrlich–Schwoebel barrier in the context of thin film growth.[37,38] Thus, because the surface of the disordered layers becomes rough and holey upon heating, the micropancakes grow while avoiding the holes, resulting in deformation of the three-phase contact line from circular to zigzag. We summarize the proposed mechanism of the formation of the zigzag micropancakes on the holey layers in Fig. 2.

As mentioned above, the surface of the micropancakes is smooth because of the aforementioned effect of surface tension. However, as shown in Fig. 1(c and d), a small number
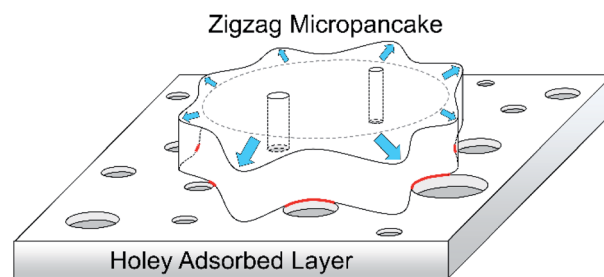

Fig. 2 Schematic image of a micropancake growing on a disordered layer while avoiding the holes, resulting in the zigzagged shape. The circles indicate the holes. The red curved lines indicate the three-phase contact line pinned at the edges of the holes.

of holes appeared even in the micropancakes after heating without being filled by the mobile gas molecules. We therefore assume that the holes reach and penetrate the underlying solid-like air layers, which cannot be filled by the constituent gas molecules because of the aforementioned Ehrlich–Schwoebel barrier. We also propose two possible formation mechanisms for the holes in the micropancakes. One is the same as those created in the disordered layers, namely due to the desorption of the adsorbed molecules described above. Because micropancakes themselves might inhibit the desorption of gas molecules from the underlying disordered layers, the number of holes in them should be smaller than in the disordered layers, which agree with our observation. The other is the coalescence of the growing micropancakes while avoiding the holes in the underlying disordered layers, which could be observed by investigating the temporal evolution of the gas domains after heating as shown in Fig. 3(d–f), which is described later.

To reinforce our interpretation and provide further insights, we investigated the time evolution of the interfacial gas phases before and after heating. Fig. 3(a–c) shows the HOPG/pure water interface before heating. Many micropancakes were observed in Fig. 3(a). After 22 minutes (Fig. 3(b)), the two micropancakes numbered 7 and 8 spontaneously moved and then coalesced into a larger one (number 10). The larger ones numbered 11, 12, 13, and 14 were also formed by the coalescences in 55 minutes (Fig. 3(c)). These mobility and spontaneous coalescence are consistent with the representative features of the micropancakes reported in the past reports.[19,24,25] In addition, several holes indicated by the green arrows in Fig. 3(c) were created in the disordered layers without heating, although they did not exist in Fig. 3(a and b) and the number of them was significantly smaller than those observed after heating. Therefore, it can be considered that this creation of fewer holes might be caused by the interaction between the AFM probe and the adsorbed gases. This result indicates that the formation of a large number of the holes shown in Fig. 1(c) is induced by heating, not a time-dependent change. Furthermore, we found that the contour of the micropancake 14 in Fig. 3(c) is deformed along the surrounding holes indicated by the green arrows. This result supports our prediction that the micropancakes grow while avoiding the holes, resulting in the deformation of the contour from circular to zigzag.

As shown in Fig. 3(d), the edge of the micropancakes deformed to zigzag-shaped and the disordered layers became rough and holey after heating, which is the same result as seen in Fig. 1. However, in contrast to the results before heating, the spontaneous movement of the micropancakes was not observed. This is because the holes and roughness of the surrounding disordered layers prevented them from moving, which agrees with our interpretation. Furthermore, we could
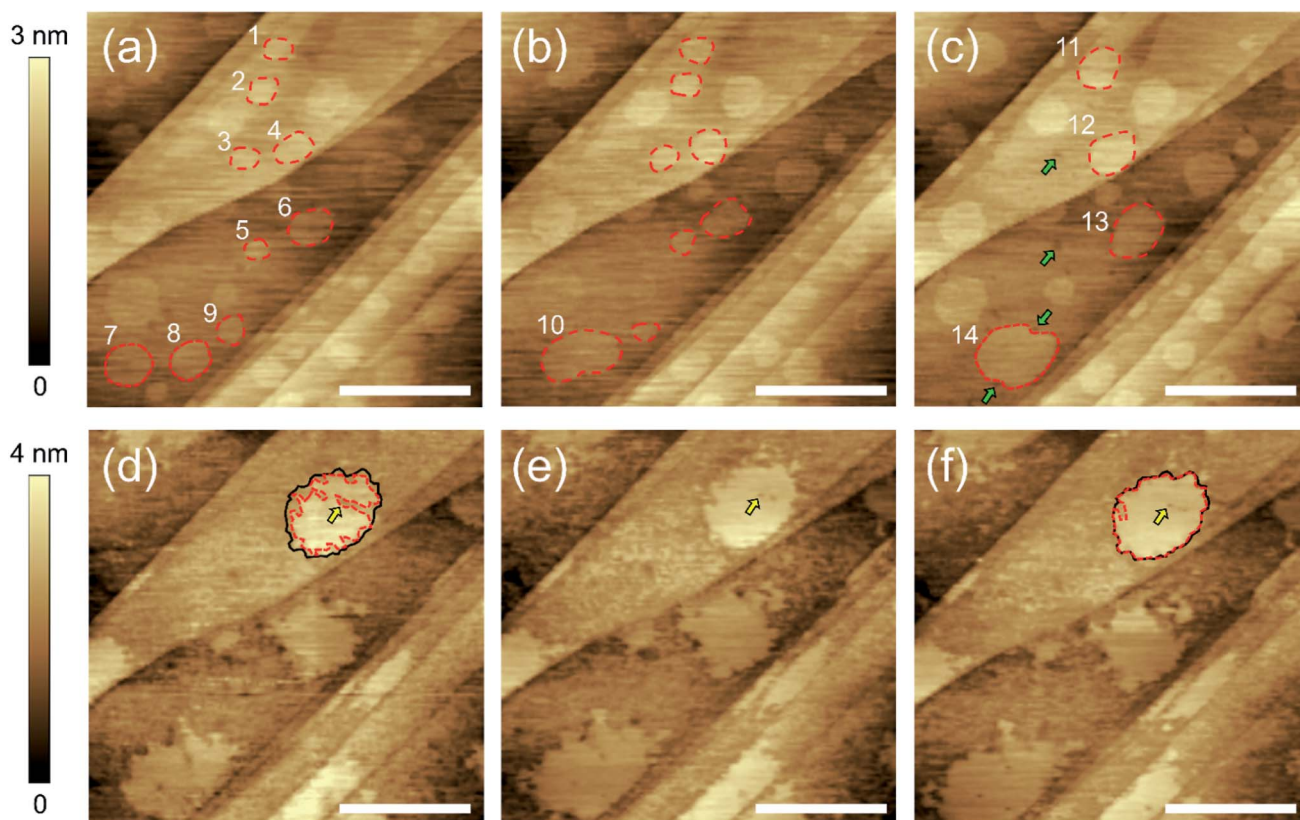
Fig. 3 Height images (3 μm × 3 μm) of the micropancakes and disordered layers (a–c) before and (d–f) after heating. The scale bars are 1 μm. (b) and (c) were measured 22 and 55 minutes after the acquisition of (a), respectively. The green arrows indicate the holes created without heating. (e) and (f) were also obtained 37 and 56 minutes after the acquisition of (d). The red broken lines and black lines indicate the contour of the micropancakes and disordered layers, respectively. The yellow arrows indicate the holes created in the interfacial layers.

observe the growth of the zigzag micropancake. First, the micropancake indicated by the red broken line in Fig. 3(d) was smaller than the underlying disordered layer indicated by the black line. In Fig. 3(e and f), its three-phase contact line expanded to the edges of the underlying disordered layers with time. During this growth, the hole in the disordered layer indicated by the yellow arrows in Fig. 3(d–f) was not filled but surrounded by the growing gas phase, resulting in the hole in the micropancake. This is the unambiguous evidence to prove our hypothesis that the holes in the micropancakes penetrate the underlying disordered layer and thus cannot be filled by the gas molecules due to the Ehrlich–Schwoebel barrier.

The binding energy of the graphite/gas interface (which is of the order of 100 meV)[16] is almost the same or even lower than that of graphite/water[32] and mica/water interfaces.[33] However, we observed self-affine rough growth arising from the low mobility of the accumulated molecules for the adsorption of gas molecules, in contrast with previous studies looking at the adsorption of water vapor on graphite and mica surfaces.[27,34] We propose two possible explanations for this discrepancy. One is the presence of the graphene coating. Previous studies on the condensation of water thin films at ambient conditions have used monolayer graphene as a cover film to prevent the water adlayers from evaporating.[27,34,35] In such experiments, water molecules are intercalated between the graphene and the underneath substrate through the edges and cracks of the graphene.[39] Because the growth of the water adlayers is only mediated by the surface diffusion of the intercalated water molecules, the growth is limited to the lateral direction. Therefore, self-affine rough growth resulting from the strong adsorption on the top of the adlayers does not occur. The second possible explanation relates to the effect of hydration structures. We proposed in our recent study that the ordered and disordered layers are stabilized by their confinement in hydration structures constructed by the surrounding water molecules, such as gas hydrates.[21] Accordingly, the gas molecules at water/solid interfaces may become immobile relative to the water molecules at gas/solid interfaces, resulting in self-affine rough growth.

Although the surface nanobubbles have been identified to be composed of gas molecules by several methods,[40,41] the origin of the thinner interfacial layers on the graphite surface, which is the most important open issue, is an ongoing debate. For example, An et al. proposed that micropancakes are derived from PDMS lubricant applied to plastic syringes and recommended to use the clean glass syringe.[42] It has been also reported that the stripe structures, which are similar to the ordered layers, are formed by the adsorption of airborne hydrocarbon contaminant.[43–45] Although we tried to acquire the Raman shifts of the micropancakes and adsorbed layers to determine the component of them, no peaks derived from them were observed because they are too thin and sparse to be detected by the Raman spectroscopy (see ESI Note S6†). However, Hwang's group have showed the strong relationship between the nucleation of the interfacial domains and the dissolved gas concentration in water.[4,16–18] Moreover, it was reported that water protects the graphite surface from the airborne hydrocarbon contaminant.[46] Our past reports have also confirmed that the interfacial domains including the nanobubbles, micropancakes, and adsorbed layers are indeed gas phases by using different techniques, such as responses to load forces applied by the AFM probe,[28] injection of degassed water,[19] and force curve measurements.[21] Furthermore, we confirmed that the interfacial domains were not nucleated on the HOPG surface in air and in degassed water, which also imply that they are composed of air molecules (see ESI Note S7†). From these results, we have confidence that they are composed of air molecules, not contaminant. We expect that further identification of these layers by different techniques from AFM, such as tip-enhanced Raman spectroscopy and scanning tunneling microscopy, will provide further insights and address this question.

Conclusions

We investigated the formation and growth processes of gas phases at HOPG/pure water interfaces induced by heating. It was found that heating promotes the formation of micropancakes that have a zigzag-shaped three-phase contact line, as well as disordered layers with a large number of holes. Furthermore, by comparing the AM-AFM images obtained before and after heating, we found that condensed gas layers grew in a SK manner. The unique growth regimes were explained in terms of thin film growth, which depends on the mobility of the constituent molecules. Specifically, the disordered layers grew only in the vertical direction in a self-affine random rough manner owing to the immobility of the strongly adsorbed molecules. By contrast, the mobile micropancakes grew in both the vertical and horizontal directions while avoiding the holes and dents of the underlying disordered layers, leading to the formation of the zigzag shape. This is because micropancakes cannot move past the edges of the disordered layers owing to the pinning effect (i.e. the Ehrlich–Schwoebel barrier). These experimental findings provide valuable insight into the physics of the adsorbed layers of air molecules at solid/liquid interfaces.

Conflicts of interest

There are no conflicts to declare.

Acknowledgements

References

1 P. G. De Gennes, *Langmuir*, 2002, **18**, 3413–3414.

2 I. Schlesinger and U. Sivan, *J. Am. Chem. Soc.*, 2018, **140**, 10473–10481.

3 D. A. Doshi, E. B. Watkins, J. N. Israelachvili and J. Majewski, *Proc. Natl. Acad. Sci. U. S. A.*, 2005, **102**, 9458–9462.

4 C.-K. Fang, H.-C. Ko, C.-W. Yang, Y.-H. Lu and I.-S. Hwang, *Sci. Rep.*, 2016, **6**, 24651.

5 N. N. Nguyen, A. V. Nguyen, K. M. Steel, L. X. Dang and M. Galib, *J. Phys. Chem. C*, 2017, **121**, 3830–3840.

6 H. Peng, M. A. Hampton and A. V. Nguyen, *Langmuir*, 2013, **29**, 6123–6130.

7 S.-T. Lou, Z.-Q. Ouyang, Y. Zhang, X.-J. Li, J. Hu, M.-Q. Li and F.-J. Yang, *J. Vac. Sci. Technol., B: Microelectron. Nanometer Struct.–Process., Meas., Phenom.*, 2000, **18**, 2573–2575.

8 N. Ishida, T. Inoue, M. Miyahara and K. Higashitani, *Langmuir*, 2000, **16**, 6377–6380.

9 C. L. Owens, E. Schach, M. Rudolph and G. R. Nash, *RSC Adv.*, 2018, **8**, 35448–35452.

10 X. Zhang, D. Y. C. Chan, D. Wang and N. Maeda, *Langmuir*, 2013, **29**, 1017–1023.

11 B. M. Borkent, S. M. Dammer, H. Schonherr, G. J. Vancso and D. Lohse, *Phys. Rev. Lett.*, 2007, **98**, 204502.

12 X. Zhang, H. Lhuissier, C. Sun and D. Lohse, *Phys. Rev. Lett.*, 2014, **112**, 144503.

13 J. R. T. Seddon, H. J. W. Zandvliet and D. Lohse, *Phys. Rev. Lett.*, 2011, **107**, 116101.

14 J. H. Weijs and D. Lohse, *Phys. Rev. Lett.*, 2013, **110**, 054501.

15 D. Lohse and X. Zhang, *Phys. Rev. E: Stat., Nonlinear, Soft Matter Phys.*, 2015, **91**, 031003.

16 Y.-H. Lu, C.-W. Yang, C.-K. Fang, H.-C. Ko and I.-S. Hwang, *Sci. Rep.*, 2014, **4**, 7189.

17 Y.-H. Lu, C.-W. Yang and I.-S. Hwang, *Appl. Surf. Sci.*, 2014, **304**, 56–64.

18 Y.-H. Lu, C.-W. Yang and I.-S. Hwang, *Langmuir*, 2012, **28**, 12691–12695.

19 H. Teshima, Y. Takata and K. Takahashi, *Appl. Phys. Lett.*, 2019, **115**, 071603.

20 C. W. Yang, K. Miyazawa, T. Fukuma, K. Miyata and I. S. Hwang, *Phys. Chem. Chem. Phys.*, 2018, **20**, 23522–23527.

21 H. Teshima, Q. Y. Li, Y. Takata and K. Takahashi, *Phys. Chem. Chem. Phys.*, 2020, **22**, 13629–13636.

22 H.-C. Ko, W.-H. Hsu, C.-W. Yang, C.-K. Fang, Y.-H. Lu and I.-S. Hwang, *Langmuir*, 2016, **32**, 11164–11171.

23 H.-S. Liao, C.-W. Yang, H.-C. Ko, E.-T. Hwu and I.-S. Hwang, *Appl. Surf. Sci.*, 2018, **434**, 913–917.

24 X. H. Zhang, N. Maeda and J. Hu, *J. Phys. Chem. B*, 2008, **112**, 13671–13675.

25 X. H. Zhang, X. Zhang, J. Sun, Z. Zhang, G. Li, H. Fang, X. Xiao, X. Zeng and J. Hu, *Langmuir*, 2007, **23**, 1778–1783.

26 J. R. T. Seddon, E. S. Kooij, B. Poelsema, H. J. W. Zandvliet and D. Lohse, *Phys. Rev. Lett.*, 2011, **106**, 056101.

27 J. Song, Q. Li, X. Wang, J. Li, S. Zhang, J. Kjems, F. Besenbacher and M. Dong, *Nat. Commun.*, 2014, **5**, 1–8.

28 H. Teshima, K. Takahashi, Y. Takata and T. Nishiyama, *J. Appl. Phys.*, 2018, **123**, 054303.

29 R. P. Berkelaar, E. Dietrich, G. A. M. Kip, E. S. Kooij, H. J. W. Zandvliet and D. Lohse, *Soft Matter*, 2014, **10**, 4947–4955.

30 H. Teshima, T. Nishiyama and K. Takahashi, *J. Chem. Phys.*, 2017, **146**, 014708.

31 H. Ibach, *Physics of surfaces and interfaces*, Springer, 2006.

32 T. Werder, J. H. Walther, R. L. Jaffe, T. Halicioglu and P. Koumoutsakos, *J. Phys. Chem. B*, 2003, **107**, 1345–1352.

33 M. Odelius, M. Bernasconi and M. Parrinello, *Phys. Rev. Lett.*, 1997, **78**, 2855–2858.

34 K. Xu, P. Cao and J. R. Heath, *Science*, 2010, **329**, 1188–1191.

35 M. J. Lee, J. S. Choi, J. S. Kim, I. S. Byun, D. H. Lee, S. Ryu, C. Lee and B. H. Park, *Nano Res.*, 2012, **5**, 710–717.

36 M. J. Rost, L. Jacobse and M. T. M. Koper, *Nat. Commun.*, 2019, **10**, 1–7.

37 G. Ehrlich and F. G. Hudda, *J. Chem. Phys.*, 1966, **44**, 1039–1049.

38 R. L. Schwoebel and E. J. Shipsey, *J. Appl. Phys.*, 1966, **37**, 3682–3686.

39 X. Feng, S. Maier and M. Salmeron, *J. Am. Chem. Soc.*, 2012, **134**, 5662–5668.

40 X. H. Zhang, A. Quinn and W. A. Ducker, *Langmuir*, 2008, **24**, 4756–4764.

41 S. R. German, X. Wu, H. An, V. S. J. Craig, T. L. Mega and X. Zhang, *ACS Nano*, 2014, **8**, 6193–6201.

42 H. An, G. Liu and V. S. J. Craig, *Adv. Colloid Interface Sci.*, 2015, **222**, 9–17.

43 D. S. Wastl, A. J. Weymouth and F. J. Giessibl, *ACS Nano*, 2014, **8**, 5233–5239.

44 A. Temiryazev, A. Frolov and M. Temiryazeva, *Carbon*, 2019, **143**, 30–37.

45 S. Seibert, S. Klassen, A. Latus, R. Bechstein and A. Kühnle, *Langmuir*, 2020, **36**, 7789–7794.

46 Z. Li, A. Kozbial, N. Nioradze, D. Parobek, G. J. Shenoy, M. Salim, S. Amemiya, L. Li and H. Liu, *ACS Nano*, 2016, **10**, 349–359.